Microscopical Damage Mechanisms in Glass Fiber Reinforced Polypropylene

J. LINDHAGEN, L. BERGLUND

Division of Polymer Engineering, Luleå University of Technology, S-971 87 Luleå, Sweden

Received 16 July 1997; accepted 27 December 1997

ABSTRACT: The damage mechanisms in two structurally different glass mat reinforced polypropylene materials were studied. *In situ* microscopy was applied during the tensile testing of thin notched sheets. Micrographs of the damage processes in the two materials are presented. The major points of damage initiation were transversely oriented fibers and fiber bundles. In the swirled mat material, cracks grew along the fiber bundles; crack formation and growth was relatively unaffected by macroscopical stress concentration. In the short fiber material, crack growth occurred at the notch. In both materials the maximum load was determined by the fibers oriented in the longitudinal direction. The different damage mechanisms were interpreted in terms of damage zone size. © 1998 John Wiley & Sons, Inc. J Appl Polym Sci 69: 1319–1327, 1998

Key words: composite; glass fiber; polypropylene; glass mat thermoplastics; microscopy; failure mechanisms

INTRODUCTION

Glass mat thermoplastics (GMTs) are used to manufacture large components with limited load-bearing capacity. Low price, low weight, and good corrosion resistance combined with good mechanical properties and short cycle times in manufacturing have secured a market, particularly for automotive components. The materials are usually made from common thermoplastics such as polypropylene (PP) or polyamide (PA) reinforced with a glass fiber mat. The mechanical properties of GMT materials were studied by Ericson and Berglund,[1] Karger–Kocsis et al.,[2–5] and Mallick,[6] among others. Studies of damage processes are important because they provide information about the underlying mechanisms for toughness, strength properties, and notch sensitivity. Kander and Siegmann studied damage processes in thin specimens of long discontinuous fiber reinforced PP.[7] A miniature tensile stage and optical microscopy were used to study the damage processes *in situ* during tensile testing. Acoustic emission was also employed, and specific acoustic signals could be assigned to damage events viewed under the microscope. Karger–Kocsis et al. studied the toughness of compact tension specimens of short fiber reinforced injection-molded PP and swirled mat PP-GMT.[5] Optical microscopy, acoustic emission, and infrared thermography were employed. Damage processes were observed, and damage zone size was determined for the two materials. Investigations of damage processes were performed by various researchers[8–15] in short fiber reinforced injection-molded thermoplastics by different methods such as fractography, acoustic emission, and *in situ* SEM observation of bending tests.

Research has shown that the toughness of GMT and long fiber reinforced thermoplastics is related to the size of the damage zone in front of a growing crack.[5,16] In the present investigation the damage processes in thin sheets of two structurally different PP based GMT materials were studied. *In situ*

Correspondence to: J. Lindhagen.

Journal of Applied Polymer Science, Vol. 69, 1319–1327 (1998)
 CCC 0021-8995/98/071319-09

optical microscopy was used during tensile tests. The objective was to identify the damage mechanisms related to the different fiber architectures with special emphasis on damage zone creation.

EXPERIMENTAL

Materials

Two glass mat reinforced PP materials with different fiber architectures were used. The swirled mat material was manufactured by Symalit AG, and it has fiber reinforcement in the form of looped continuous fiber bundles. It is manufactured by a melt impregnation process where layers of continuous swirled mat are laminated with layers of PP film in a band press. The fiber content is 33% by weight, which corresponds to 15% by volume. The short fiber material was manufactured by Ahlstrom Glassfibre Ltd., and it has evenly distributed single fibers of 12 mm length with random fiber orientation. It is manufactured by a wet slurry deposition method similar to paper making. Its fiber content is 40% by weight or 19% by volume.

Experiments

Sheets of the two materials were cut into small 15 × 15 mm pieces with a band saw. A flat mold with a surface area of 50 × 100 mm was placed in an oven and heated to 235°C. A piece of either material was placed inside the mold. The mold was then placed in a cold platen press and closed. The pressure on the mold surface was 20 MPa. The results were thin sheets of GMT with a thickness of approximately 0.17 mm for the swirled mat material and 0.20 mm for the short fiber material. Tensile specimens were cut from the thin sheets; the dimensions are shown in Figure 1. Central circular hole notches with a diameter of 2 mm were punched. The objective of the notches was to create an initiation point for damage to facilitate the microscopy studies. The specimens were tested in a Minimat miniature tensile stage mounted in a Zeiss Axioplan microscope. Tensile tests were performed with a crosshead speed of 1.15 mm/min. The specimens were studied in transmitted white light. The tensile tests were interrupted at desired intervals and micrographs were taken with a 35 mm camera using black and white negative film. The presented micrographs were assembled from numerous small micrographs and rephotographed because the whole specimens could not be studied during testing. This technique of micrograph assembly creates some visual problems. In the presented micrographs the observant reader may observe thin lines that emanate from the border between two original micrographs. It can also be difficult to follow certain fibers over a longer distance because they may present sideways jumps at the border between two original micrographs.

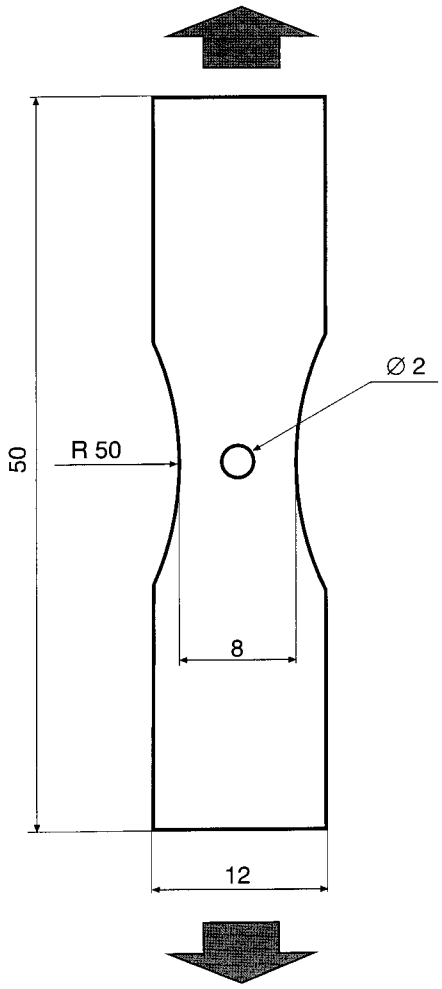

Figure 1 The dimensions of the thin tensile specimens (mm).

RESULTS AND DISCUSSION

Swirled Mat Material

Figure 2 shows the central part of a tensile specimen of the swirled mat material in different states of damage. In Figure 2(a) the specimen is un-

loaded. The bundle structure of the swirled mat material is evident. Fiber bundles containing numerous parallel fibers are separated by areas with a few single fibers. Thus, the variation in local fiber content and fiber orientation distribution is significant on a microlevel. The fiber diameter is around 20 μm, as measured in the micrographs. The initial damage mechanism can be detected in Figure 2(b). The specimen here carries a load of 25 N. Black shadows appear along a number of fiber bundles that are oriented transverse to the direction of loading. The shadows indicate that debonding occurred. The major points of damage initiation are fiber bundles with transverse orientation to the direction of loading. Damage is prevented in areas with an abundance of longitudinal fibers, because the reinforcement effect of longitudinal fibers prevents the local deformation that is necessary to initiate debonding. Stress concentrations cause an increase in damage. However, transversely oriented fiber bundles are generally more prone to debond than transversely oriented single fibers located in highly stressed areas. Therefore, damage is first initiated at transverse fiber bundles and only later around stress concentrations such as the notch. Consequently, there are two different kinds of initial damage points in the swirled mat material. In the present specimen, the two kinds of damage initiation points coincide. In general, the damage in the swirled mat material may or may not occur close to the notch, depending on the fiber structure of the particular specimen. Debonding of transverse fibers as the initial damage mechanism in GMT materials was also observed by Kander and Siegmann[7] and by Karger–Kocsis et al.[5] Sjögren and Berglund observed simultaneous debonding and initiation of plastic matrix deformation in PP-glass bead composites.[17]

The initial debonding of transverse fibers permits plastic deformation of the surrounding matrix. The load increases on neighboring fibers. The second stage is debonding of fibers oriented at off-axis angles to the direction of loading. When such fibers have debonded along their full length, the load in the damaged zone is taken up by the fibers oriented in the longitudinal direction. Debondings propagate easily along fibers that are not crossed by longitudinal fibers and coalesce through the thickness of the specimen to form microcracks.

Cracks in the swirled mat material first form in transverse fiber bundles located at the edge of the specimen or at the notch and with a limited number of bridging longitudinal fibers. In Figure 2(c) a crack has opened at the notch edge. The crack follows a fiber bundle and is unbridged by longitudinal fibers. At this stage the specimen carries its maximum load of 40 N. Substantial damage is observed between the notch and the specimen edge. Regions with matrix plasticity appear as dark areas in the micrographs. This is due to so-called stress whitening, which is strain-induced crystallization of the PP matrix material. The stress whitened areas do not transmit light, which causes the dark appearance of the specimen.

Growth of debondings, as well as crack growth, along transverse fiber bundles is hindered by crossing longitudinal fibers and bundles. Also, the local strain induced by crack or debond growth causes redistribution of stresses in the specimen, which may initiate damage and crack growth at another location in the specimen. Therefore, the swirled mat material displays a large damage zone caused by a number of local damage zones. The loads in the damage zones are taken up by the longitudinal fibers. These longitudinal fibers break at some location when the fiber stress exceeds the fiber strength, and then they show debonding. The fracture of longitudinal fibers allows significant local strain and thus permits a crack to also form in regions where the longitudinal fibers initially prevented crack formation. Thomason et al.[18] showed that the ultimate failure of these materials is governed by the fibers. The cracks in the swirled mat material preferably propagate along transversely or diagonally oriented fiber bundles by internal debonding and bundle separation or by a mechanism where the fibers inside a bundle move relative to each other by shearing. Figure 2(d) shows how the initial unbridged open crack has stopped propagating and crack growth has been redirected. The load on the specimen has gone down to 30 N. Cracks originating at the specimen edge have opened beside the original crack. Damage has also been initiated at the other side of the notch where a large zone of matrix plasticity can be observed. It is interesting to note how far damage has developed on one side of the notch before it is initiated on the other side. Debondings can also be observed at the upper side of the unaffected specimen.

Crossing fiber bundles often do not fracture at the point where a growing crack crosses.[19] Therefore, the growing crack deviates in the swirled mat material. The final crack exhibits sideways jumps as a result of the crack deviation process. The resultant fracture surface on a full-scale tensile specimen is very uneven. This is clearly de-

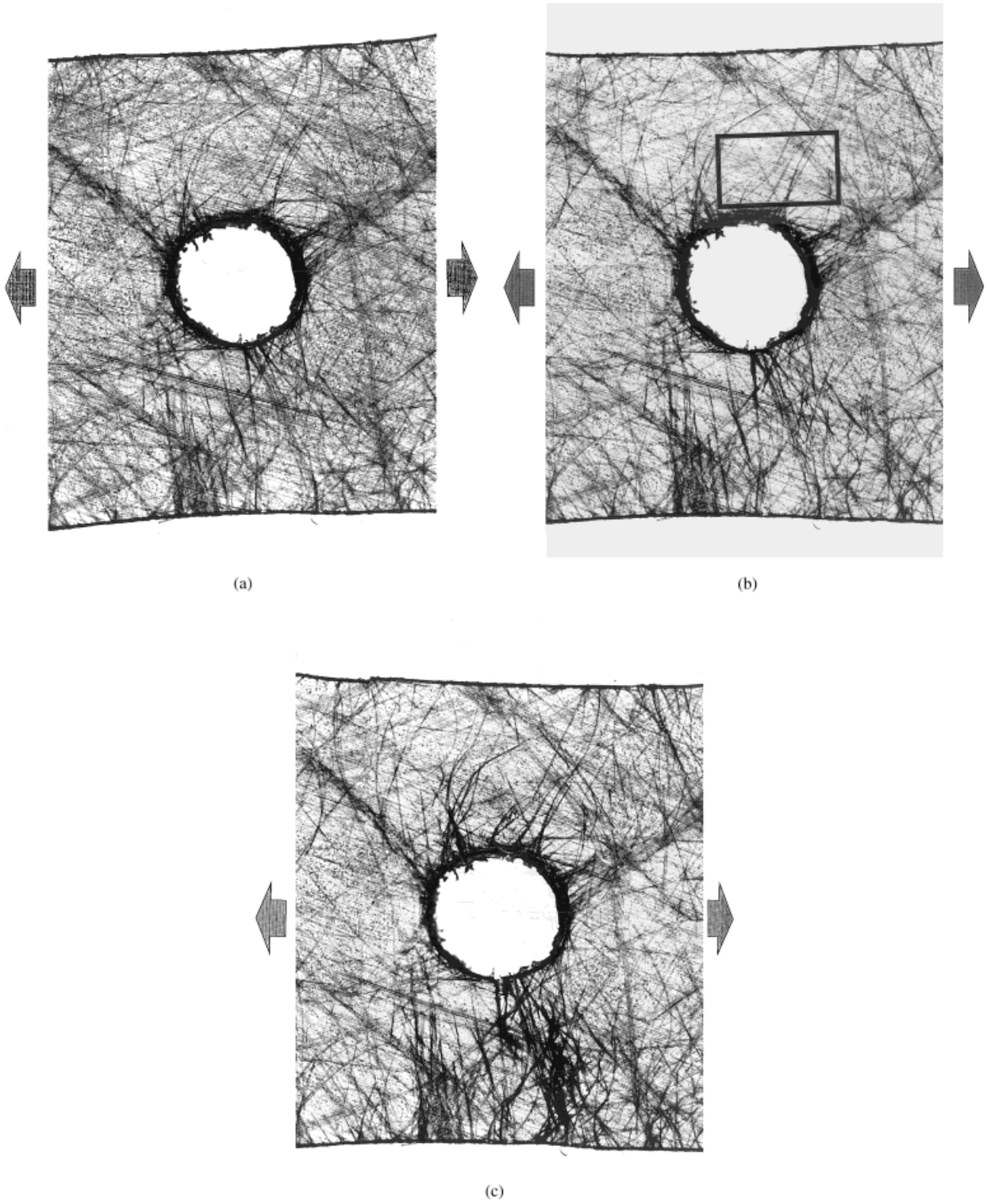

Figure 2 A specimen of the swirled mat material at different states of damage.

picted in Ericson and Berglund.[1] Long-range debonding and splitting up of transverse fiber bundles in the swirled mat material was observed by Karger–Kocsis et al.[5]

In Figure 2(e) the cracks have propagated throughout the specimen. Bridging fibers can be seen in Figure 2(d,e). These fibers have already failed or debonded along their full length and are

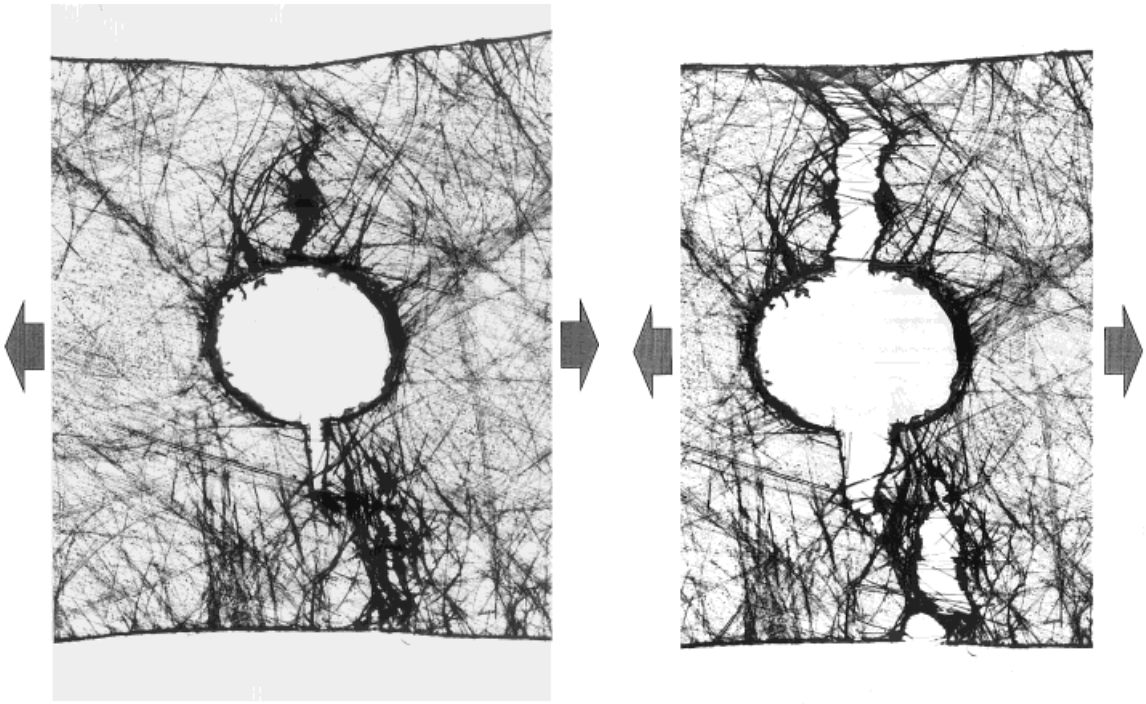

Figure 2 (*Continued from the previous page*)

in the process of being pulled out of the matrix. A section of matrix material and broken fibers, which continue to deform plastically, can be seen bridging the crack. The matrix plastic deformation involved in crack widening has been described in Kander and Siegmann.[7] Some of the bridging fibers are bent, and some are in the process of changing direction and curvature as they are being pulled. This change in position of the fibers upon crack extension was also observed by Karger–Kocsis et al.[5]

The process of failure of longitudinal fibers followed by crack formation in the swirled mat material can be followed in detail in Figure 3. They are enlargements of a small region of the specimen shown in Figure 2. The region is located just above the notch, as indicated by the rectangle in Figure 2(b). In Figure 3(a) the region is shown in the undamaged state. Figure 3(b) shows the region at the stage depicted in Figure 2(c) where the specimen carries maximum load. At three locations, denoted by arrows, failures of fibers oriented along the direction of loading have occurred. The failures have occurred where other fibers cross. In the left part of the pictures grey shades can be seen. They are caused by the beginning of matrix stress whitening and indicate that matrix plastic deformation has initiated. Debonding of transverse fibers can also be observed.

When the longitudinal fibers break, they debond along their full length and start to pull out of the matrix. This is seen in Figure 3(c) in which the fiber failures in Figure 3(b) have grown to dark tunnels left empty by the fibers. The micrograph is an enlargement of Figure 2(d) in which the load has started to decrease. Substantial damage, the preamble of crack formation, has occurred in the left part of the picture. The crack growth accompanied by further fiber pull-out can be observed in Figures 3(d,e).

Short Fiber Material

The damage and fracture processes in the short fiber material are shown in Figure 4. In the micrographs, the differences in fiber architecture compared to the swirled mat material are clearly seen. There is also a difference in fiber diameter and fiber length between the materials. The fiber diameter was 11 μm for the short fiber material. Furthermore, the higher fiber volume fraction of the short fiber material is evident, although the difference in fiber volume fraction is exaggerated in the micrographs for two reasons: because the

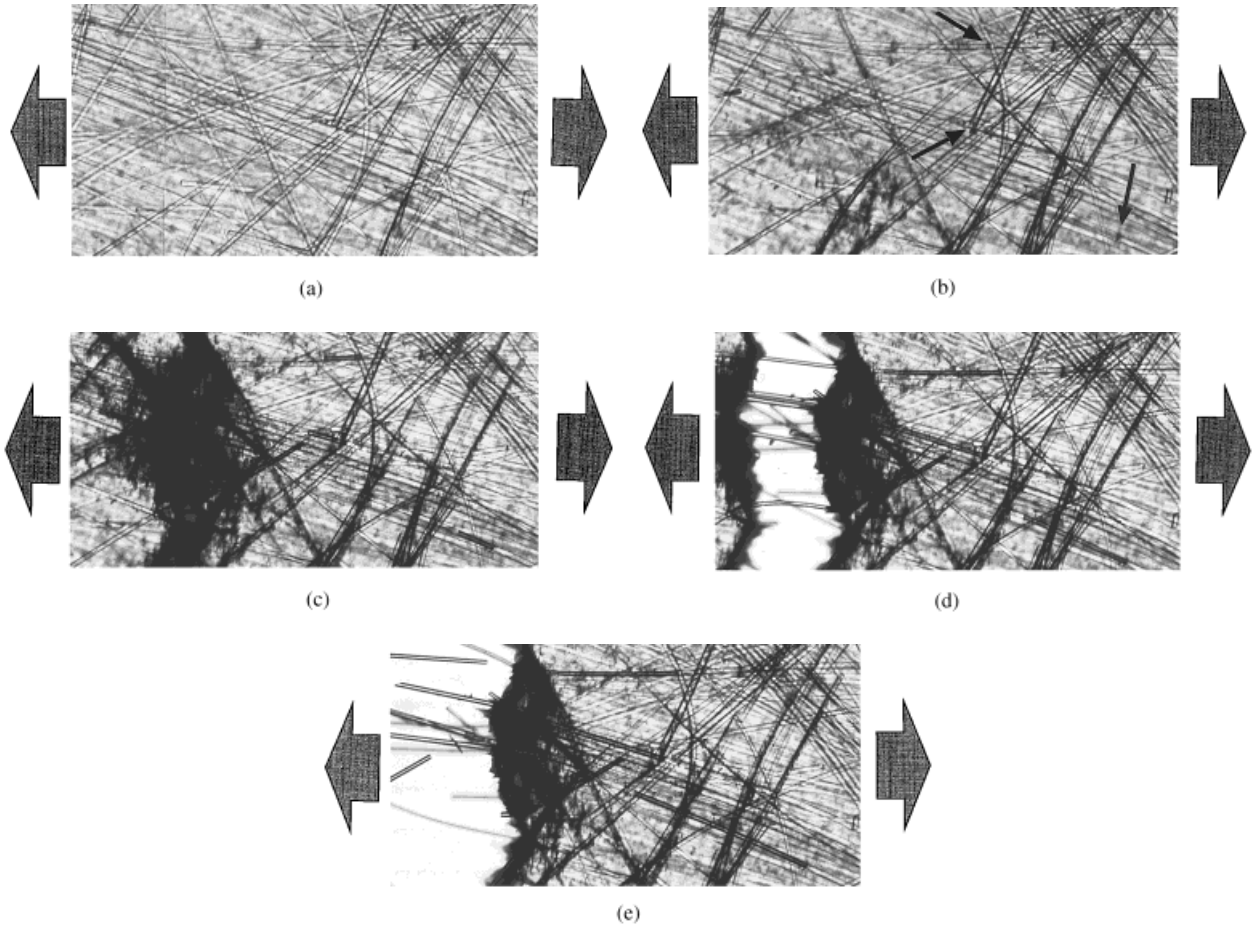

Figure 3 The fiber fracture and crack formation process in the swirled mat material.

fiber diameter and length is larger in the swirled mat material, the fibers are fewer than in the short fiber material for a given volume fraction; and the concentration of fibers in fiber bundles in the swirled mat material creates an optical illusion that there are fewer fibers, because areas with low fiber content exist.

The short fiber material has single fibers evenly distributed throughout the material; see Figure 4(a), which depicts a specimen in the unloaded state. Then consider Figure 4(b). It is taken at the point of maximum load at 90 N. The overall impression of the micrograph is that the specimen has become uniformly darker compared to Figure 4(a). This shows that damage is more evenly distributed. As in the swirled mat material, the initial damage is debonding of fibers oriented transverse to the direction of loading. Because there are no fiber bundles present in the short fiber material, debondings occur at a later stage than in the swirled mat material and are more evenly distributed throughout the material volume.

Due to the stress concentration, further damage in the short fiber material is concentrated in the area around the notch. Crack formation in the short fiber material is depicted in Figure 4(c). At this stage the load on the specimen has started to decrease. A crack has formed in the damage zone close to the notch and has grown diagonally to the specimen edges. The diagonal growth direction indicates a diagonally oriented region of lower material strength, although this is not evident from the micrograph. Due to the absence of fiber bundles as initiation points, crack formation in the short fiber material occurs at a later stage than in the swirled mat material. The damage state in the whole specimens has developed more before crack growth commences, and more strain energy is stored in the specimen. Therefore, crack growth in the short fiber material is a rapid process and is difficult to capture at an intermediate

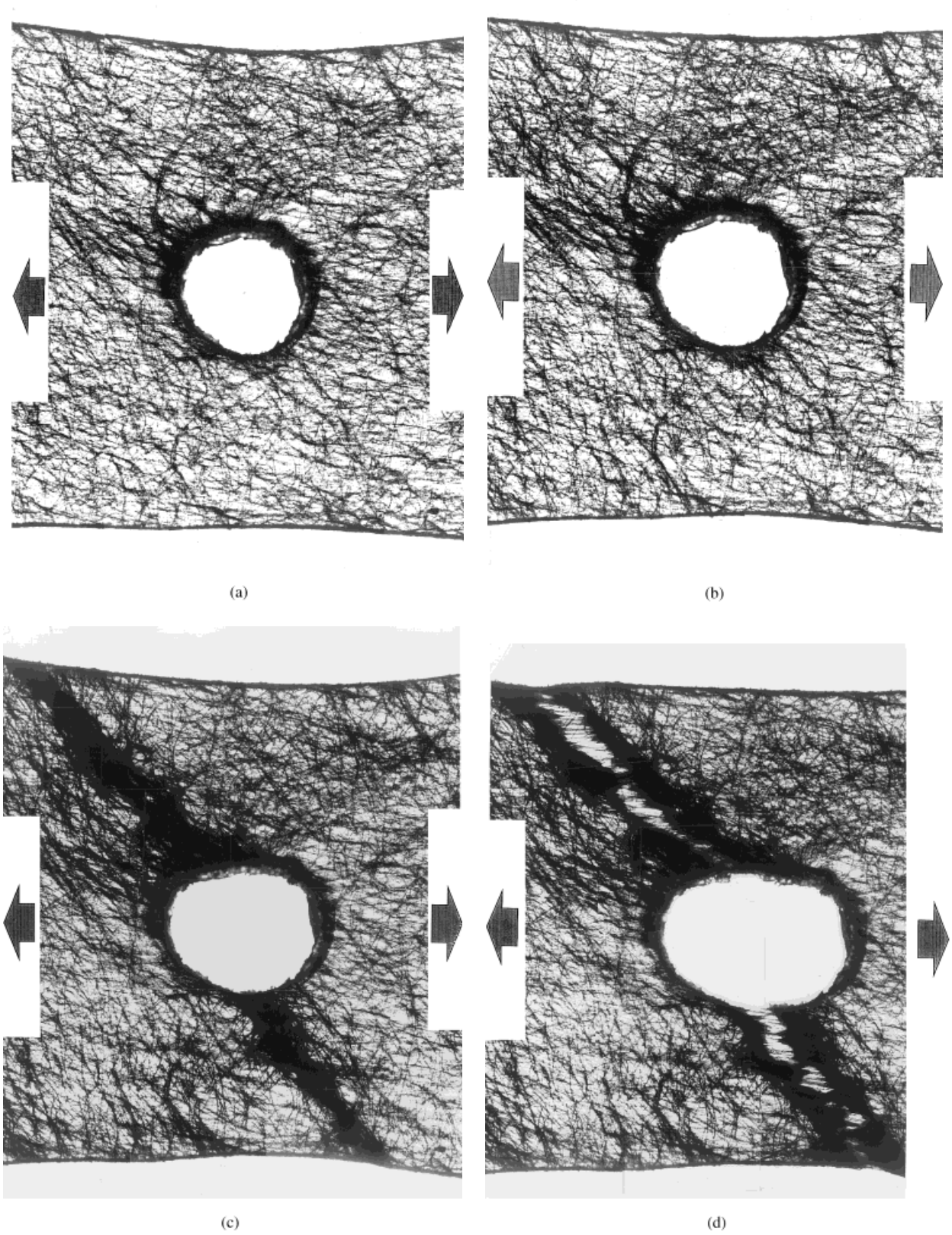

Figure 4 A specimen of the short fiber material at different states of damage.

stage. However, Thomason et al. showed that the strength of various GMT materials with different fiber lengths is governed by the fiber strength.[18] Therefore, there is no reason to believe that crack formation in the short fiber material is not controlled by failure of the longitudinal fibers. This is supported by the fact that the load starts to decrease simultaneously with major crack formation.

In the short fiber material the single fibers oriented in longitudinal direction offer less resistance to crack growth compared to the fiber bundles of the swirled mat material. The absence of fiber bundles gives no preferred pathways for crack growth and no crack deviation. Therefore, the crack will propagate relatively smoothly to the specimen edge; a smaller material volume is involved in and affected by the crack growth process compared to the swirled mat material. As a result, the short fiber material exhibits a smaller damage zone size. Bridging fibers in the process of pull-out during crack growth in the short fiber material can be observed in Figure 4(d).

Material Differences

The initial damage mechanism is debonding of fibers oriented transverse to the direction of loading. Subsequently, debonding and pull-out of fibers more aligned with the direction of loading occurs, combined with plastic deformation of the matrix. When longitudinal fibers start to break and pull out, significant local strains are allowed and a crack is formed. The crack propagates along transverse and diagonal fibers by debonding or shearing mechanisms of fibers that lie close and parallel to each other. Final failure is governed by fracture and pull-out of longitudinal fibers. The swirled mat material has a bundle structure where concentrations of fibers lying parallel and close to each other are common. Fiber bundles oriented transverse to the direction of loading act as initiation points for damage. Massive debonding occurs within fiber bundles, and the fibers tend to separate. Cracks are formed within and grow along the fiber bundles. Longitudinal crossing fiber bundles effectively stop a growing crack from further propagation. Thus, the crack is forced to deviate or crack growth is initiated elsewhere and a large damage zone is created in the swirled mat material. The short fiber material exhibits a more uniform fiber architecture with single fibers evenly distributed. Damage is initiated equally at different fibers with transverse orientation throughout the material. The presence of the notch causes a concentration of damage. A crack is then formed in the damage zone near the notch equator. It propagates in a straightforward manner relatively unhindered by crossing single fibers. The damage zone in the short fiber material is smaller compared to the swirled mat material.

CONCLUSIONS

Thin notched tensile specimens of two structurally different GMT materials were tested in a miniature tensile stage. The specimens were simultaneously studied in an optical microscope. Micrographs were presented that exhibited the differences in microstructure and damage processes in the two materials. Damage initiation occurred at fiber bundles or single fibers oriented transverse to the direction of loading. When fiber bundles were present, they provided a natural pathway for crack growth. On the other hand, crossing fiber bundles stopped or deviated the crack. As a consequence, a large material volume was involved in energy dissipation during crack growth in the swirled mat material. For the short fiber material, the absence of fiber bundles provided no inherent initiation points for crack formation. Instead a uniform damage state was created throughout the material. Crack formation occurred in areas of stress concentration. During crack growth a smaller material volume was active in energy dissipation in the short fiber material, partly because of the smaller resistance to crack growth from single fibers.

REFERENCES

1. M. Ericson and L. Berglund, *Compos. Sci. Technol.,* **43,** 269 (1992).
2. R. Schledjewski and J. Karger–Kocsis, *J. Thermoplast. Compos. Mater.,* **7,** 270 (1994).
3. J. Karger–Kocsis and Zs. Fejes–Kozma, *J. Reinf. Plast. Compos.,* **13,** 768 (1994).
4. J. Karger–Kocsis and Zs. Fejes–Kozma, *J. Reinf. Plast. Compos.,* **13,** 822 (1994).
5. J. Karger–Kocsis, T. Harmia, and T. Czigany, *Compos. Sci. Technol.,* **54,** 287 (1995).
6. P. K. Mallick, in *Proceedings of the 8th Advanced Composites Conference,* Chicago, IL, 1992, ASM International, Materials park, 1992, p. 203.
7. R. G. Kander and A. Siegmann, *Polym. Compos.,* **13,** 154 (1992).
8. N. Sato, T. Kurauchi, S. Sato, and O. Kamigaito, *J. Mater. Sci.,* **19,** 1145 (1984).

9. N. Sato, T. Kurauchi, S. Sato, and O. Kamigaito, in *Fracture Mechanics,* M. F. Kanninen and A. T. Hopper, Eds., ASTM Special Technical Publication (STP) 868, American Society for Testing and Materials, Philadelphia, PA, 1985.
10. N. Sato, T. Kurauchi, S. Sato, and O. Kamigaito, *J. Mater. Sci.,* **26,** 3891 (1991).
11. J. Karger–Kocsis and K. Friedrich, *Compos. Sci. Technol.,* **32,** 293 (1988).
12. D. E. Spahr, K. Friedrich, J. M. Schultz, and R. S. Bailey, *J. Mater. Sci.,* **25,** 4427 (1990).
13. T. Harmia and K. Friedrich, *Compos. Sci. Technol.,* **53,** 423 (1995).
14. J. Denault, T. Vu–Khanh, and B. Foster, *Polym. Compos.,* **10,** 313 (1989).
15. T. Vu–Khanh and J. Denault, in *The 37th International SAMPE Symposium,* Anaheim, CA, 1992, SAMPE, Covina, CA, 1992, p. 579.
16. J. Lindhagen and L. Berglund, *Polym. Compos.,* **18,** 40 (1997).
17. B. A. Sjögren and L. A. Berglund, *Polym. Compos.,* **18,** 1 (1997).
18. J. L. Thomason, M. A. Vlug, G. Schipper, and H. G. L. T. Krikor, *Composites,* **27A,** 1075 (1996).
19. J. A. Holmberg, *J. Reinf. Plast. Compos.,* **11,** 1302 (1992).